International Journal of Computer Information Systems and Industrial Management Applications
ISSN 2150-7988 Volume 18(21s) 2026 pp. 316-327
https://doi.org/10.70917/ijcisim-2026-5297
Article

COUPLED OPTIMIZATION OF DEFECT DENSITY, ABSORBER PROPERTIES, AND INTERFACES FOR HIGH-PERFORMANCE PEROVSKITE SOLAR CELLS: A SCAPS-1D STUDY

Shrutika Sharma[1], Amit Saxena[2]

[1,2]Department of science, Oriental University, Indore (M.P.), India
[1]Correspondence Author: shrutikasharma452012@gmail.com

Abstract: The optimization of defect density is a critical factor governing the photovoltaic performance of perovskite solar cells. The SCAPS-1D simulation results demonstrate that reducing the bulk trap density from 10^{15} to 10^{10} cm^{-3} substantially improves the device performance by suppressing trap-assisted non-radiative recombination and enhancing the effective lifetime of photogenerated charge carriers. The reduced recombination rate facilitates efficient carrier transport and collection, resulting in improvements in the open-circuit voltage (Voc), short-circuit current density (Jsc), fill factor (FF), and power conversion efficiency (PCE). These findings emphasize the importance of defect passivation and improved material quality for achieving high-performance perovskite photovoltaic devices. However, the beneficial effects associated with lower bulk defect densities can be limited by imperfections present at the semiconductor surface and heterointerfaces. Surface contamination and interfacial defects may generate localized electronic states that act as recombination centers and adversely influence charge extraction. Such imperfections can lead to undesirable phenomena, including Fermi-level pinning and enhanced recombination losses, thereby reducing the potential performance improvement obtained through bulk defect reduction. Therefore, effective surface and interface engineering is essential for maintaining favorable energy-level alignment and minimizing carrier losses. The comprehensive SCAPS-1D analysis further confirms that the photovoltaic performance of perovskite solar cells depends on the simultaneous optimization of multiple device parameters. An appropriate absorber bandgap is necessary for efficient solar-spectrum utilization, whereas an optimized absorber thickness provides sufficient optical absorption without introducing excessive recombination losses. Similarly, low defect density improves carrier lifetime, while carefully controlled donor and acceptor concentrations promote efficient charge separation and transport. The results indicate that these parameters are strongly interdependent and should be optimized collectively rather than independently. Overall, the study demonstrates that the combined optimization of absorber bandgap, thickness, defect density, doping concentration, and interfacial properties provides an effective pathway toward achieving enhanced photovoltaic performance and improved device efficiency in perovskite solar cells.

Keywords: Perovskite solar cells; SCAPS-1D simulation; defect density; trap-assisted recombination; photovoltaic performance; absorber optimization; carrier lifetime; interface engineering; doping concentration; power conversion efficiency

1. INTRODUCTION

These intrinsic optoelectronic characteristics enable perovskite solar cells (PSCs) to deliver high short-circuit current density (JSC) together with a favorable open-circuit voltage (VOC), resulting in power conversion efficiencies comparable to those of established silicon-based photovoltaic technologies [1]. Continued improvements in PSC efficiency and operational stability have been achieved through compositional engineering, including the

incorporation of formamidinium and cesium cations, mixed-halide systems, and other tailored perovskite formulations. In parallel, the development of advanced device configurations, such as planar, mesoporous, and tandem architectures, has further expanded the performance potential of these devices [2]. Because experimental fabrication requires considerable time and resources, numerical simulation has become an important complementary approach for investigating the influence of material and device parameters before laboratory implementation [3].

Device simulations provide a systematic framework for examining the relationship between physical parameters and photovoltaic characteristics, particularly the current density–voltage (J–V) response and the associated performance indicators. This approach can reduce extensive trial-and-error experimentation and assist in identifying suitable operating and design ranges. Previous simulation studies have demonstrated that absorber thickness strongly influences optical absorption, carrier generation, and recombination processes within PSCs [4]. Increasing the thickness initially improves photon absorption and consequently enhances JSC. However, once sufficient light absorption is achieved, further increases in thickness may increase carrier transport distances and recombination losses, leading to reductions in VOC, fill factor (FF), and overall power conversion efficiency (PCE) [10].

The absorber bandgap is another key parameter controlling device performance. Compositional modification of the perovskite material can alter the bandgap and establish a trade-off between photocurrent generation and photovoltage. Materials with narrower bandgaps generally absorb a broader portion of the solar spectrum and can produce higher JSC, whereas wider-bandgap absorbers can support higher VOC [5]. Similarly, bulk defects and interfacial trap states significantly affect carrier recombination and can limit both VOC and FF by introducing non-radiative loss pathways [6]. Therefore, improving material quality and applying effective defect-passivation strategies can substantially enhance device efficiency [7].

Doping concentration also plays an important role in determining charge transport and electric-field distribution within PSCs. Although perovskite absorbers are commonly lightly doped [8], excessive doping can promote additional recombination mechanisms, including Auger recombination, and increase carrier scattering [9]. Consequently, an optimum doping range is required for maximum performance. Reported SCAPS studies have demonstrated significant improvements through the optimization of doping and defect density [11]. Overall, the present simulation methodology provides guidance for experimental development by identifying critical parameters, particularly defect density, absorber thickness, band alignment, and doping concentration, that offer the greatest potential for improving PSC efficiency.

2. Methodology

To evaluate the influence of different device parameters, a baseline perovskite solar cell (PSC) structure was developed using SCAPS-1D based on previously reported high-performance devices. The simulated architecture consisted of FTO/TiO_2/$CH_3NH_3PbI_3$/Spiro-OMeTAD/Au, representing the front contact, electron transport layer, absorber, hole transport layer, and back contact, respectively. Material parameters, including bandgap, electron affinity, dielectric constant, and carrier mobility, were selected from published experimental and simulation studies. The $MAPbI_3$ absorber was assigned a bandgap of approximately 1.55 eV. Bulk and interface defect states were incorporated to evaluate recombination effects and carrier transport behavior within the device.

Using this baseline, we performed a series of SCAPS simulations, each varying one parameter while keeping others fixed. Key parameters studied include:

(1) **Absorber band gap (Eg)** – adjusted by hypothetically changing perovskite composition (e.g. mixing bromide for higher Eg or tin for lower Eg.

(2) **Absorber thickness** – varied from thin (200–300 nm) to thick (1500–2000 nm) to capture the transition from incomplete absorption to full absorption and onset of recombination loss.

(3) **Defect density** – the bulk trap density in the perovskite was varied over orders of magnitude (1014 to 1017 cm−3), and interface defect densities were also adjusted in some cases (1010 to 1015 cm−2) to evaluate their impact on *V*OC and FF.

(4) **Doping concentration** – the majority carrier density in the perovskite (acceptor density for p-type) was increased from ~1014 up to 1018 cm−3, which is a range spanning intrinsic or lightly doped to moderately heavily doped semiconductors. In certain simulations, we also adjusted doping in the transport layers (e.g. TiO2 doping for better conductivity) to observe any additional effects.

PCE for each parameter set. The trends were then plotted and tabulated (as partially shown in Tables 1 and 2). To ensure reliability, the SCAPS model included realistic considerations such as interface band offsets, series resistance (from contacts), and, where relevant, non-ideal effects like surface recombination and shunt paths. For instance, a small series resistance (a few ohms) was included to mimic electrode and transport layer resistance, which can slightly reduce FF at high currents. Radiative recombination and Auger recombination were included for completeness in some simulations: radiative recombination is intrinsic in direct band gap materials like perovskites and sets an upper limit on *V*OC (the radiative limit), while Auger recombination can become significant at very high doping levels or carrier injection. The SRH (Shockley-Read-Hall) recombination via defect traps was modeled as the dominant non-radiative mechanism, with lifetimes inversely proportional to trap density. The parameter variations in SCAPS were done one at a time (one-factor-at-a-time approach) to isolate each effect, although in reality these parameters can be coupled (e.g. changing composition affects both band gap and defect density). We therefore later discuss interplay where relevant, based on literature that examines combined effects.

It should be noted that simulation results can differ from experimental values due to idealizations (e.g. uniform defect distribution, sharp interfaces). However, the trends and relative sensitivities from SCAPS provide valuable qualitative and semi-quantitative guidance. The next section presents the results and discussion for each parameter's influence, referencing both our simulation outcomes and recent published studies for validation and comparison.

3. Results and Discussion

The Shockley–Queisser detailed-balance model places the theoretical efficiency limit of a single-junction solar cell near 33% under radiative-limit conditions [12]. Perovskite solar cells with bandgaps around 1.5–1.6 eV, particularly $MAPbI_3$ (~1.55 eV), therefore operate within a favorable range and have demonstrated efficiencies approaching 25–26% [13]. Bandgap engineering involves an inherent trade-off between JSC and VOC. Increasing Eg generally enhances VOC but restricts photon absorption, reducing JSC [14]. Conversely, reducing Eg extends spectral response toward longer wavelengths and increases JSC, although it may decrease VOC and increase thermalization losses [15].

4. Effect of Absorber Band Gap

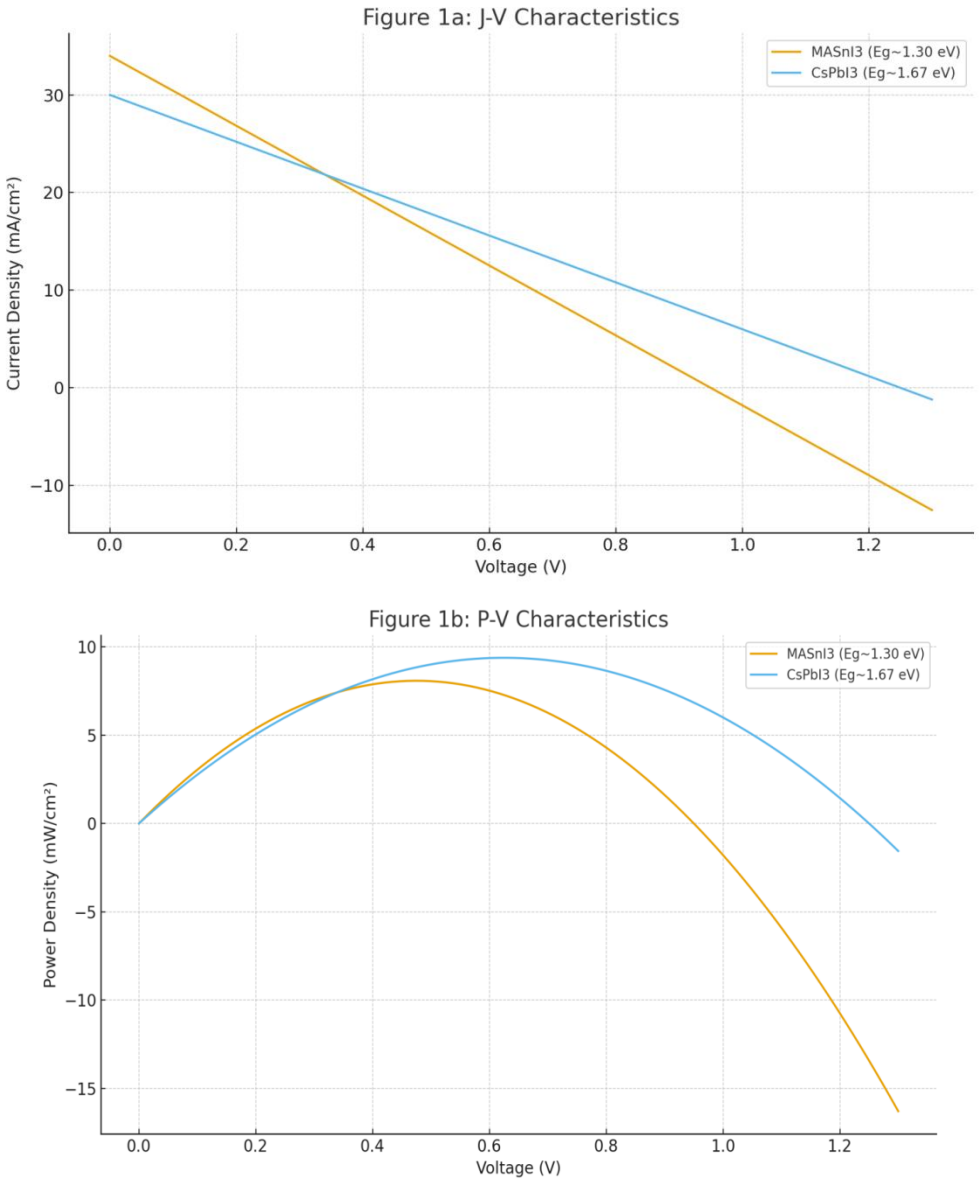

Figure 1 illustrates this trade-off through comparative SCAPS-1D simulations of two PSC configurations, highlighting the corresponding variation in JSC and VOC with absorber bandgap.

The influence of absorber bandgap on photovoltaic performance was further examined by comparing perovskite compositions with substantially different optical bandgaps. As illustrated in Figure 1, the $MASnI_3$ absorber, with a bandgap of approximately 1.30 eV, provides an extended spectral response and consequently produces a relatively high JSC. However, the corresponding VOC is lower because of the smaller energetic separation between the conduction and valence bands [16]. In comparison, $CsPbI_3$, with a bandgap of approximately 1.67 eV, exhibits a higher attainable photovoltage because of its larger bandgap. Under comparable simulated conditions, the increase in VOC can compensate for the reduction in photocurrent, resulting in improved overall PCE. Mahmoud et al. reported a simulated PCE of approximately 22.86% for $CsPbI_3$, with a VOC of about 1.24 V, whereas $MASnI_3$ produced approximately 21–22% efficiency with a VOC close to 0.95 V [16].

The ratio between VOC and the absorber bandgap also provides an indication of voltage losses associated with non-radiative recombination. For $CsPbI_3$, the simulated VOC corresponds to approximately 74% of its bandgap, indicating comparatively favorable carrier recombination characteristics. The corresponding value for $MASnI_3$ is approximately 73%, although the lower bandgap enables stronger photon harvesting and higher current generation. These results demonstrate that increasing the bandgap does not necessarily guarantee a higher PCE because the resulting voltage enhancement must be balanced against the loss in photocurrent.

The optimum bandgap is also strongly dependent on the radiative efficiency and defect characteristics of the absorber [18]. Pazos-Outón et al. showed that perovskite materials with very high internal photoluminescence quantum efficiency can approach favorable voltage limits because non-radiative recombination losses are strongly suppressed [19]. For single-junction PSCs, $MAPbI_3$, with a bandgap of approximately 1.55 eV, represents a useful compromise between photon absorption and photovoltage [20]. Wider-bandgap compositions in the range of approximately 1.7–1.8 eV are particularly attractive for tandem photovoltaic architectures, where they can serve as wide-gap top absorbers. However, their reduced absorption of long-wavelength photons generally limits the JSC and single-junction PCE [21].

In contrast, narrow-bandgap Sn–Pb perovskites can generate substantial photocurrent because their absorption extends further into the near-infrared region. Nevertheless, these materials commonly exhibit reduced VOC, particularly when defect-assisted recombination is significant. Consequently, the increase in JSC may not be sufficient to compensate for voltage losses, resulting in a lower overall PCE [22]. From the perspective of single-junction operation, absorber bandgaps within approximately 1.3–1.6 eV therefore provide a practical balance between current generation and voltage output. Compositional engineering, such as controlling the FA/MA ratio and halide composition, provides an effective means of tuning the bandgap over a broad range and selecting compositions appropriate for specific photovoltaic architectures [23].

Overall, the SCAPS-1D results indicate that VOC generally increases with increasing bandgap, whereas JSC decreases because fewer lower-energy photons can contribute to photocurrent generation. The resulting PCE therefore exhibits an optimum region rather than a continuous increase with bandgap. A modest increase in bandgap may be advantageous when it produces a significant voltage gain without excessive current loss. However, the practical benefit of a wider bandgap depends strongly on suppressing bulk and interfacial non-radiative recombination. Effective defect passivation, high-quality crystallinity, and suitable charge-transport layers are consequently essential for converting the theoretical voltage advantage of wide-bandgap perovskites into measurable efficiency gains [46]. Under well-controlled bulk and interface conditions, wide-bandgap PSCs can approach their attainable voltage limits [50,51]. Conversely, narrow-bandgap absorbers require careful control of recombination and material quality to retain their high photocurrent advantage.

5. Effect of Absorber Layer Thickness

The absorber thickness strongly influences the optical and electrical characteristics of perovskite solar cells. An excessively thin absorber may not utilize the incident solar spectrum effectively, particularly near the band-edge region where the absorption coefficient is relatively low. Conversely, increasing the absorber thickness enhances photon absorption and initially improves JSC; however, excessive thickness can increase bulk recombination and carrier-transport losses. Therefore, an optimum thickness is required to achieve a favorable balance between light harvesting and charge collection.

As presented in Table 1, SCAPS-1D results for $MASnI_3$ show that increasing the absorber thickness from 300 to 2000 nm increases JSC from approximately 28.7 to 35.1 mA cm^{-2}, with the photocurrent approaching saturation beyond about 1000 nm. In contrast, VOC decreases from nearly 0.998 to 0.909 V because of increasing recombination losses. The maximum PCE of approximately 26.2% is obtained at an absorber thickness of about 600–700 nm [4,58]. Between 300 and 700 nm, the substantial increase in JSC outweighs the relatively small reduction in VOC. Beyond this range, further thickness provides limited optical benefit while increasing recombination. Photocarriers generated deep within the absorber may recombine before reaching the selective contacts, particularly when the absorber

thickness exceeds the effective carrier diffusion length. Thus, thickness optimization is essential for achieving maximum PSC efficiency.

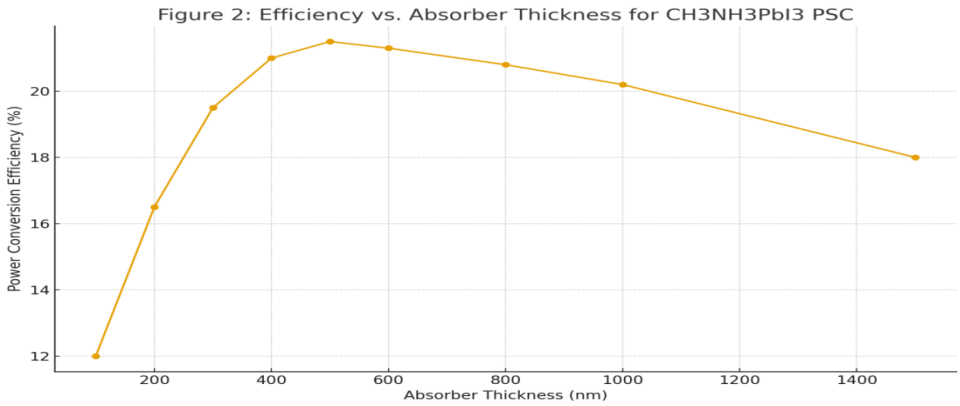

Figure 2 presents the simulated dependence of photovoltaic efficiency on absorber thickness for a planar $CH_3NH_3PbI_3$ perovskite solar cell. The results reported by Niaei et al. demonstrate a rapid increase in PCE as the absorber thickness increases from approximately 200 nm, followed by a broad maximum in the 400–600 nm region [25,26].

An optimum thickness of nearly 500 nm produced a PCE of approximately 15%, compared with about 11% at 200 nm and 13% at 1000 nm. These results indicate that insufficient absorber thickness restricts photon absorption and limits photocurrent generation, whereas excessive thickness provides only marginal optical benefits while increasing recombination losses.

A similar thickness dependence was reported by Liu and Kelly, who identified approximately 300 nm as a favorable thickness for planar PSCs. Their analysis showed that very thin films exhibited inadequate light absorption and carrier collection, while further increases in thickness produced only relatively small changes in device efficiency. The precise optimum, therefore, depends on the optical absorption coefficient, carrier diffusion length, and charge-collection characteristics of the device.

Perovskite materials with long carrier diffusion lengths can potentially support thicker absorber layers without severe recombination losses. However, practical polycrystalline films generally exhibit diffusion lengths ranging from several hundred nanometers to approximately 1 μm, making absorber thickness an important design parameter. Excessive thickness may also increase the transport distance for photogenerated carriers and contribute to resistive losses. Jeyakumar et al. observed that increasing the $MAPbI_3$ thickness from 300 to 600 nm substantially enhanced JSC, whereas increasing it to 1000 nm provided little additional photocurrent while reducing VOC by approximately 30 mV. These observations support the existence of an efficiency plateau beyond the optimum thickness.

Overall, both simulation and experimental investigations indicate that an absorber thickness of approximately 400–800 nm provides a practical balance between photon absorption and carrier collection for many lead-based PSCs. Within this range, sufficient optical absorption can be achieved while limiting bulk recombination and transport losses. Thus, thickness optimization, together with improvements in crystallinity, defect passivation, and carrier diffusion length, is essential for achieving high-performance PSCs.

Table 1. The simulated results indicate that an absorber thickness of approximately 600–700 nm provides the maximum PCE. Further thickness increases lead to greater recombination, reducing VOC and FF despite limited gains in JSC. The simulation uses TiO_2 as ETL, Spiro-OMeTAD as HTL, 10^{15} cm^{-3} doping and defect density, at 300 K.

Absorber Thickness	**VOC (V)**	**JSC (mA/cm²)**	**FF (%)**	**PCE (%)**

300 nm	0.998	28.74	82.99	23.8
700 nm	0.960	33.83	80.64	26.2
1000 nm	0.943	34.63	78.53	25.6
1500 nm	0.923	34.99	74.83	24.2
2000 nm	0.909	35.06	70.88	22.6

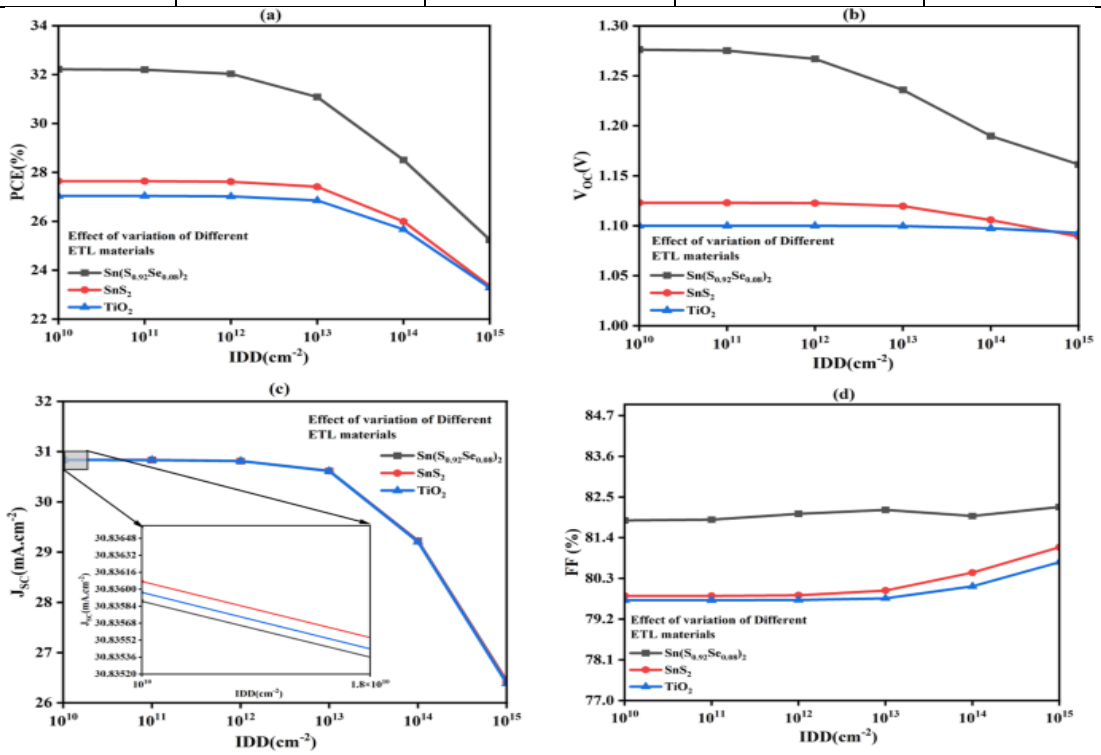

Figure 1. Effect of absorber bandgap on J–V characteristics. (a) Simulated J–V responses of $MASnI_3$ (Eg ≈ 1.30 eV) and $CsPbI_3$ (Eg ≈ 1.67 eV) PSCs, illustrating the higher VOC and slightly reduced JSC for the wider-bandgap absorber. (b) Corresponding power-density curves, showing the superior maximum power output of the $CsPbI_3$ device. Adapted from Mahmoud et al. (2023) [1].

Effect of Bulk and Interface Defect Density on PSC Performance

Defect density is one of the most influential parameters governing the photovoltaic performance of perovskite solar cells (PSCs). Excessive defect states within the absorber introduce additional non-radiative recombination pathways, which increase carrier losses and reduce the attainable open-circuit voltage (*V*OC). The associated increase in recombination current can also deteriorate the fill factor (FF), particularly when defects are distributed throughout the absorber layer [24]. Defects located at the interfaces between the electron transport layer (ETL), perovskite absorber, and hole transport layer (HTL) can be equally detrimental. Dangling bonds, vacancies, and chemically imperfect interfaces provide additional recombination sites and interfere with efficient charge extraction. Consequently, increasing bulk or interface defect density moves the device further away from its radiative-limit performance and reduces the achievable power conversion efficiency (PCE) [25].

In SCAPS-1D, the absorber quality can be evaluated by systematically varying the bulk trap density (*N*t) [26]. A reduction in *N*t from 10^{16} to 10^{14} cm^{-3} generally produces a noticeable increase in *V*OC, together with improvements in *J*SC and FF. Conversely, when the defect concentration approaches 10^{16} cm^{-3}, enhanced trap-assisted recombination can reduce *V*OC below 0.9 V and restrict the PCE to approximately 14%. These results demonstrate the strong sensitivity of PSC performance to absorber quality. Interface defect density (IDD) also has a pronounced influence.

Reported simulations of optimized $FASnI_3$ devices showed that increasing IDD by several orders of magnitude reduced *V*OC from approximately 1.28 to 1.16 V and decreased PCE from 32.2% to 25.2%, while FF remained close to 82% [27]. This behavior indicates that interface defects can primarily influence voltage losses when the bulk absorber has relatively low defect density.

The influence of bulk defects on FF can be more substantial because recombination occurs across the absorber volume and modifies the shape of the *J–V* response [28]. Ansari *et al.* reported a reduction in simulated PCE from approximately 22% to 14%, accompanied by a decrease in FF from nearly 81% to 72%, when the combined defect density was increased [29]. Their results further indicated that ETL/perovskite interface defects become particularly important after bulk defect concentrations have been reduced. Thus, improving absorber crystallinity alone may not be sufficient; efficient interface passivation and appropriate energy-level alignment are also required [30].

Defect control can be achieved through bulk and surface passivation, improved precursor stoichiometry, optimized solvent processing, and incorporation of suitable chemical additives. Surface treatments based on ammonium halides can suppress interfacial recombination and improve *V*OC, while additives such as KI and thiophene-derived compounds can reduce detrimental bulk trap states. Tin-based perovskites require particular attention because Sn^{2+} oxidation can generate vacancy-related defects and contribute to substantial voltage losses [31]. Chemical reduction, compositional modification, and controlled processing can therefore assist in reducing their defect density.

Overall, SCAPS-1D analysis demonstrates that minimizing both bulk and interface defects is essential for obtaining high-efficiency PSCs. At sufficiently low bulk trap densities, interface quality becomes a major limiting factor, as also indicated by simulation-based optimization studies. Effective defect engineering can consequently reduce non-radiative voltage losses and enable PSCs to approach their theoretical efficiency limits [32,33].

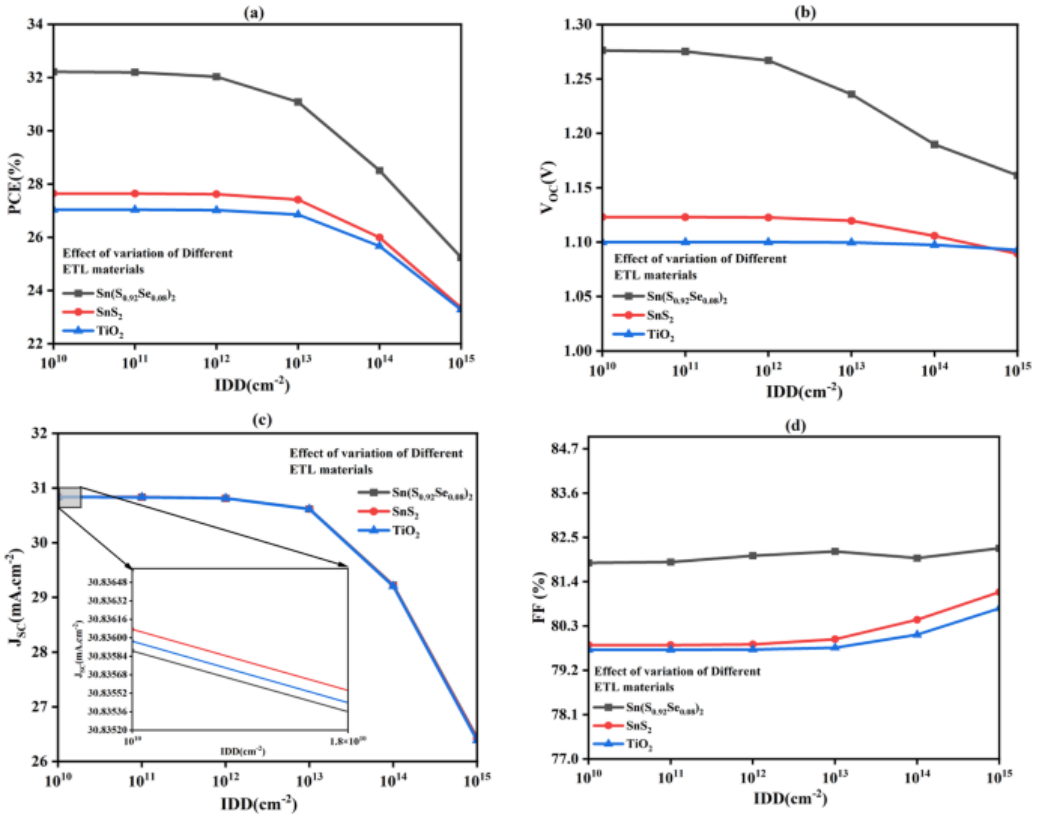

Figure 3. Impact of interface defect density on PSC performance.

The simulated PCE, VOC, JSC, and FF decrease progressively as interface defect density increases from 10^{10} to 10^{15} cm^{-2}. The pronounced reduction in VOC highlights the detrimental effect of interfacial recombination on device performance. Adapted from Verma and Dwivedi (2025) [5].

Effect of Absorber Doping Concentration on PSC Performance

The doping concentration of the perovskite absorber is an important parameter that influences the electrical properties and photovoltaic response of perovskite solar cells (PSCs). In most numerical models, the absorber is considered intrinsic or weakly p-type, with an acceptor concentration (NA) typically in the range of 10^{14}–10^{15} cm^{-3} [34]. Such low carrier concentrations are consistent with the relatively weak intentional doping commonly observed in perovskite films. Nevertheless, the electronic character of the absorber can be modified through compositional engineering, intentional dopants, or intrinsic defects that introduce shallow donor or acceptor states [35].

An increase in doping concentration can improve the built-in potential and modify the carrier distribution across the absorber. Under illumination, the open-circuit voltage is related to the separation of the electron and hole quasi-Fermi levels. Consequently, suitable doping can increase the attainable VOC by improving the energetic difference between the charge-selective regions [36]. Increased doping can also reduce the depletion or space-charge width within the absorber, resulting in a stronger electric field over a narrower region. This modification may facilitate charge separation and extraction and can consequently improve JSC and FF under appropriate conditions [37]. However, these benefits are not unlimited. Excessive doping may increase Auger recombination, enhance carrier–carrier scattering, and reduce the effective carrier mobility. At sufficiently high concentrations, the Fermi level can approach a band edge, producing degenerate semiconductor behavior and altering the assumptions associated with conventional carrier transport [38].

The SCAPS-1D results presented in Table 2 indicate that increasing the absorber doping concentration produces a substantial improvement in VOC, FF, and PCE over the investigated range [39]. In the $MASnI_3$ device investigated by Bouderbala and Hamdi, increasing the doping concentration from 1×10^{14} to 1×10^{18} cm^{-3} increased VOC from approximately 0.96 to 1.11 V. During the same variation, FF increased from about 80.6% to 86.6%, while PCE increased from approximately 26.2% to 30.2% [41]. The improvement in efficiency is therefore mainly associated with the enhanced voltage and fill factor. In contrast, JSC changes only slightly and may begin to decline at high doping concentrations because of increased recombination and reduced carrier-collection efficiency [40].

Experimental studies also suggest that controlled modification of the carrier concentration can improve interfacial energetics and device voltage. Moderate p-type doping may enhance band bending and reduce unfavorable barriers at charge-selective interfaces. However, the beneficial effect depends strongly on the nature and concentration of the dopant. Unlike an idealized SCAPS calculation, practical doping can introduce additional defects, impurity states, or structural changes. Dopants that generate deep electronic states may therefore increase non-radiative recombination and offset the expected improvement in carrier concentration. This distinction is particularly important when simulation results are compared with experimentally fabricated devices.

At high carrier concentrations, Auger recombination becomes increasingly relevant because it involves the interaction of three charge carriers. Bouderbala and Hamdi reported that concentrations approaching or exceeding 10^{18} cm^{-3} can produce measurable Auger-related losses, accompanied by a reduction in JSC [42]. Therefore, although heavy doping can improve VOC and FF, an excessive concentration may eventually reduce the overall efficiency. A moderate doping range of approximately 10^{16}–10^{17} cm^{-3} may consequently provide a useful compromise between enhanced electric-field strength and recombination losses, provided that additional trap states are not introduced.

The influence of unintentional doping should also be considered because native defects can modify the electronic character of perovskite absorbers. Vacancies and non-stoichiometric compositions may produce either donor- or acceptor-like behavior, resulting in self-doping of the material [43]. Experimental observations further indicate that controlled and relatively mild doping can improve VOC and FF, whereas excessive compositional

deviation may disturb carrier balance and degrade device performance. These findings emphasize that the optimum doping level is strongly dependent on absorber composition, defect density, and interface properties.

In addition to absorber doping, the conductivity and Fermi-level positions of the transport layers play an important role in determining the overall device performance. Highly doped hole-transport layers, such as doped Spiro-OMeTAD, and appropriately engineered electron-transport layers can reduce resistive losses and facilitate favorable energy alignment [46]. These modifications indirectly improve the diode characteristics and charge extraction efficiency.

Overall, the SCAPS-1D analysis indicates that controlled absorber doping can provide a significant route toward improving *V*OC, FF, and PCE [44]. The results suggest that moderately doped perovskite absorbers may outperform nearly intrinsic materials when increased carrier concentration is achieved without simultaneously generating additional recombination centers [45]. However, the practical implementation of such doping requires careful control of composition, defect formation, and interfacial properties. Therefore, optimization of absorber doping should be considered together with defect passivation and transport-layer engineering rather than as an isolated parameter.

Table 2. Increasing doping concentration improves VOC and FF through enhanced charge separation and extraction, thereby increasing PCE. At 1×10^{18} cm^{-3}, a slight JSC reduction occurs because of increased Auger recombination. Results correspond to a 600 nm absorber thickness.

Acceptor Doping (cm^{-3})	VOC (V)	JSC (mA/cm^2)	FF (%)	PCE (%)
1 × 10^14	0.960	33.83	80.64	26.21
1 × 10^15	0.962	33.85	82.32	26.82
1 × 10^16	0.991	33.67	84.10	28.06
1 × 10^17	1.045	32.53	85.22	28.98
1 × 10^18	1.107	31.49	86.63	30.21

6. Conclusion

The present SCAPS-1D investigation demonstrates that achieving high power conversion efficiency (PCE) in perovskite solar cells (PSCs) requires simultaneous optimization of absorber properties and device architecture. The absorber bandgap plays a central role in determining the balance between photocurrent and photovoltage. A bandgap in the range of approximately 1.3–1.6 eV provides a favorable compromise between *J*SC and *V*OC for single-junction PSCs. Increasing the bandgap beyond approximately 1.7 eV substantially restricts the absorption of long-wavelength photons and consequently reduces *J*SC under standard one-sun illumination. Such wide-bandgap compositions are therefore more attractive for tandem photovoltaic applications.

Absorber thickness also exhibits a distinct optimum. The simulations indicate that perovskite layers of approximately 500–700 nm can provide an effective balance between photon absorption and carrier collection. Very thin absorbers, particularly below 300 nm, show insufficient optical absorption and consequently lower photocurrent. In contrast, increasing the thickness beyond approximately 1000 nm provides limited additional current while increasing the probability of bulk recombination, resulting in reductions in *V*OC and FF. The optimum thickness may vary with absorber quality, carrier diffusion length, and light-management strategies.

Defect density represents another major limitation to PSC efficiency. Reducing bulk trap concentrations substantially improves *V*OC and, consequently, PCE by suppressing non-radiative recombination. The results further indicate that interface defects become increasingly important when bulk defects are effectively controlled. Therefore, high-quality absorber layers alone are insufficient; efficient interface passivation and suitable energy-level alignment are also necessary to minimize carrier losses and improve charge extraction.

The doping concentration of the absorber provides an additional means of controlling device performance. Moderate doping, particularly within approximately 10^{16}–10^{17} cm^{-3}, can enhance *V*OC and FF by modifying carrier distributions and internal electric fields. Nevertheless, excessive doping may introduce Auger recombination and other transport-related losses. Consequently, the desired carrier concentration should be achieved without generating additional deep-level defects.

Overall, the findings demonstrate that ultra-high PSC efficiency depends on a balanced combination of bandgap selection, absorber-thickness optimization, defect suppression, interface engineering, and controlled doping. Emerging approaches involving advanced passivation, 2D/3D perovskite structures, compositional engineering, and selective transport-layer doping offer further opportunities for reducing recombination and resistive losses. Continued integration of numerical modelling with experimental validation will be essential for translating these optimized parameters into practical high-efficiency devices. The present analysis therefore highlights SCAPS-1D as a useful predictive tool for identifying sensitive material and device parameters and establishing rational design strategies for next-generation PSCs.

REFERENCES

1. Pham, H. D., Xianqiang, L., Li, W., Manzhos, S., Kyaw, A. K. K., & Sonar, P. (2019). Organic interfacial materials for perovskite-based optoelectronic devices. Energy & Environmental Science, 12(4), 1177–1209. https://doi.org/10.1039/C8EE02744G
2. Mohamed, O. M. (2022). Perovskite solar cells engineering and characterization. https://doi.org/10.32657/10356/163116
3. Pushpakaran, B. N., & Bayne, S. B. (2019). Modeling and electrothermal simulation of SiC power devices: Using SILVACO® Atlas. World Scientific.
4. Mundt, L. E. (2018). High-resolution analysis of perovskite absorbers in photovoltaics.
5. Wei, M. (2020). Composition and dimensionality engineering of perovskite materials for photovoltaic applications.
6. He, R., et al. (2021). Wide-bandgap organic–inorganic hybrid and all-inorganic perovskite solar cells and their application in all-perovskite tandem solar cells. Energy & Environmental Science, 14(11), 5723–5759. https://doi.org/10.1039/D1EE01562A
7. Veldhuis, S. A., et al. (2016). Perovskite materials for light-emitting diodes and lasers. Advanced Materials, 28(32), 6804–6834. https://doi.org/10.1002/adma.201600669
8. Washburn, N. R. (1998). Properties of Na-doped lanthanum manganite grown in hydroxide flux.
9. Zuo, G. (2018). Doping and density of states engineering for organic thermoelectrics. Linköping University Electronic Press.
10. Elumalai, N. K., & Uddin, A. (2016). Open circuit voltage of organic solar cells: An in-depth review. Energy & Environmental Science, 9(2), 391–410. https://doi.org/10.1039/C5EE02871J
11. Han, M., & Ooka, R. (2023). Large-eddy simulation based on the lattice Boltzmann method for built environment problems. Springer Nature.
12. Re-defining photovoltaic efficiency through molecule scale control: Final report. (2015).
13. Tosado, G. A. (2020). Development of highly efficient and stable lead-free perovskite solar cells through composition and interface engineering.
14. Han, G., Zhang, S., Boix, P. P., Wong, L. H., Sun, L., & Lien, S.-Y. (2017). Towards high efficiency thin film solar cells. Progress in Materials Science, 87, 246–291. https://doi.org/10.1016/j.pmatsci.2017.02.003
15. Feng, S., Li, B., Xu, B., & Wang, Z. (2023). Hybrid perovskites and 2D materials in optoelectronic and photocatalytic applications. Crystals, 13(11), 1566. https://doi.org/10.3390/cryst13111566
16. Subhani, N. M. S., Fatima, N. A., Kokab, N. A., Riaz, N. A., & Mubashar, N. S. (2025). Perovskite solar cells and their types. Book of Collection, 2(1), 45–90. https://doi.org/10.71146/kjmr202
17. Ahmad, S., Kazim, S., & Grätzel, M. (2022). Perovskite solar cells: Materials, processes, and devices. John Wiley & Sons.
18. Dittrich, T. (2014). Materials concepts for solar cells. World Scientific Publishing.
19. De Quilettes, D. W. (2017). Probing local heterogeneity in the optoelectronic properties of organic-inorganic perovskites using fluorescence microscopy.
20. Hu, M. (2016). Wide bandgap organo-lead trihalide perovskites for solar cells.
21. 0.7-eV GaInAs junction for a GaInP: Preprint. (2006).
22. Machín, A., & Márquez, F. (2024). Advancements in photovoltaic cell materials: Silicon, organic, and perovskite solar cells. Materials, 17(5), 1165. https://doi.org/10.3390/ma17051165
23. Hardy, J. (2021). Functionalisation of lead halide perovskites with anthracene. https://doi.org/10.26686/wgtn.13888346.v1

24. Noman, M., Khan, A. H. H., & Jan, S. T. (2024). Interface engineering and defect passivation for enhanced hole extraction, ion migration, and optimal charge dynamics in both lead-based and lead-free perovskite solar cells. Scientific Reports, 14(1). https://doi.org/10.1038/s41598-024-56246-4
25. James, K. (2000). The effects of phosphonic acids in dye-sensitized solar cells. https://doi.org/10.15760/etd.2946
26. Grossiord, N., Kroon, J. M., Andriessen, R., & Blom, P. W. M. (2011). Degradation mechanisms in organic photovoltaic devices. Organic Electronics, 13(3), 432–456. https://doi.org/10.1016/j.orgel.2011.11.027
27. Howard, K. J. (2022). Degradation of Cd(Se,Te) and perovskite photovoltaic devices: A numerical simulation.
28. Xue, J. (2020). The role of surface in photovoltaic perovskites: From quantum dots to bulk thin films.
29. Li, C. (2020). Normal-, low-, and wide-bandgap perovskites and their applications in solar cells.
30. Sahare, S., et al. (2021). Emerging perovskite solar cell technology: Remedial actions for the foremost challenges. Advanced Energy Materials, 11(42), 2101085. https://doi.org/10.1002/aenm.202101085
31. Costa, R. (2023). Combination of natural betanidin dye with synthetic organic sensitiser towards dye-sensitised solar cell application. https://doi.org/10.58694/20.500.12479/2195
32. Wang, F. F. Y. (2012). Impurity doping processes in silicon. Elsevier.
33. Li, J. (2017). The investigation of molecular doping and diffusion in organic electronic materials and device structures.
34. Kaydanov, V. I., & Ohno, T. R. (2007). Studies of basic electronic properties of CdTe-based solar cells and their evolution during processing and stress: Final technical report, 16 October 2001–31 August 2005. https://doi.org/10.2172/899988
35. Bhattarai, S., et al. (2023). Designing an efficient lead-free perovskite solar cell through a computational method. Crystals, 13(8), 1175. https://doi.org/10.3390/cryst13081175
36. Kosyachenko, L. A. (2011). Solar cells: Silicon wafer-based technologies. BoD–Books on Demand.
37. Takanabe, K. (2017). Photocatalytic water splitting: Quantitative approaches toward photocatalyst by design. ACS Catalysis, 7(11), 8006–8022. https://doi.org/10.1021/acscatal.7b02662
38. Adjokatse, S. (2019). Organic-inorganic hybrid perovskites: Photophysics, thin film fabrication and solar cells. https://doi.org/10.33612/diss.95664256
39. Ultra high P-doping material research for GaN-based light emitters. (2007).
40. Azar, M. H., et al. (2023). SCAPS-empowered machine learning modelling of perovskite solar cells: Predictive design of active layer and hole transport materials. Photonics, 10(3), 271. https://doi.org/10.3390/photonics10030271
41. Jayathissa, R. (2019). Investigation of structural, optical and electronic properties of modified methylammonium lead iodide perovskites.
42. You, P., Tang, G., & Yan, F. (2018). Two-dimensional materials in perovskite solar cells. Materials Today Energy, 11, 128–158. https://doi.org/10.1016/j.mtener.2018.11.006.